

Conformal Virtual Colon Flattening

Wei Hong

Xianfeng Gu

Feng Qiu

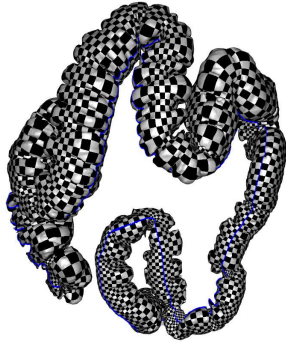
Miao Jin

Arie Kaufman

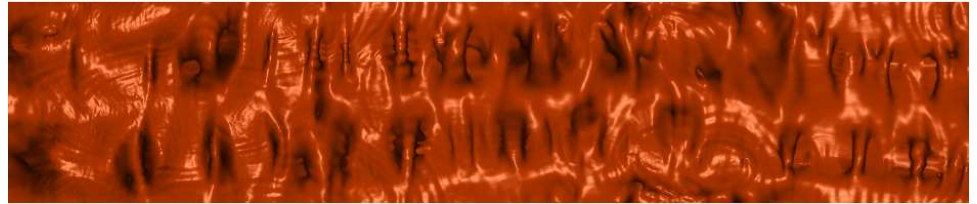
Center for Visual Computing (CVC) and Department of Computer Science *

Stony Brook University

Stony Brook, NY 11794-4400, USA



(a) Holomorphic 1-form



(b) Conformal virtual colon flattening

Figure 1: Conformal Virtual Colon Flattening: (a) illustrates the holomorphic one-form on the colon surface by texture-mapping a checkerboard image. (b) exhibits the conformal flattening induced by (a).

Abstract

We present an efficient colon flattening algorithm using conformal structure, which is angle-preserving and minimizes the global distortion. Moreover, our algorithm is general which can handle high genus surfaces. First, the colon wall is segmented and extracted from the CT dataset. The topology noise (i.e., minute handle) is located and removed automatically. The holomorphic 1-form, a pair of orthogonal vector fields, is then computed on the 3D colon surface mesh using the conjugate gradient method. The colon surface is cut along a vertical trajectory traced using the holomorphic 1-form. Consequently, the 3D colon surface is conformal mapped to a 2D rectangle. The flattened 2D mesh is then rendered using a direct volume rendering method accelerated with the GPU. Our algorithm is tested with a number of CT datasets of real pathological cases, and gives consistent results. We demonstrated that the shape of the polyps is well preserved on the flattened colon images, which provides an efficient way to enhance the navigation of a virtual colonoscopy system.

Keywords: Conformal Mapping, Direct Volume Rendering, Virtual Colonoscopy

1 Introduction

Virtual colonoscopy uses computed tomographic (CT) images of patient's abdomen and a virtual fly-through visualization system [Hong et al. 1997] that allows the physician to navigate within a 3D model of the colon searching for polyps, the precursors of cancer. Virtual colonoscopy has been successfully demonstrated to be more convenient and efficient than the real optical colonoscopy. However, because of the length of the colon, inspecting the entire colon wall is time consuming, and prone to errors. Moreover, polyps be-

hind folds may be hidden, which results in incomplete examinations.

Virtual dissection is an efficient visualization technique for polyp detection, in which the entire inner surface of the colon is displayed as a single 2D image. The straightforward method [Balogh et al. 2002; Wang and Vannier 1995] starts with uniformly resampling the colonic central path. At each sampling point, a cross section orthogonal to the path is computed. The central path is straightened and the cross sections are unfolded and remapped into a new 3D volume. The isosurface is then extracted and rendered. In this method, nearby cross sections may overlap at high curvature regions. As a consequence, a polyp might appear twice or be missed completely in the flattened image. Balogh et al. [2002] use an iterative method to correct cross sections, using two consecutive ones at a time. Wang et al. [1998; 1999] use electrical field lines generated by a local charged path to generate curved cross sections instead of planar sections. If the complete path is charged, then the cross sections tend to diverge, avoiding overlaps. However, due to the expansive computation of the global charge, the authors only locally charge the path, which cannot guarantee that the curved cross sections do not intersect each other any more.

Paik et al. [2000] have used cartographic projections to project the whole solid angle of the camera. This approach samples the solid angle of the camera, and maps it onto a cylinder which is mapped finally to the image. However, this method causes distortions in shape. Bartroff et al. [2001b] have proposed a method to move a camera along the central path of the colon. For each camera position a small cylinder tangent to the path is defined. Rays starting at the cylinder axis and being orthogonal to the cylinder surface are traced. The cylinder is then opened and mapped to a 2D image. The result is a video where each frame shows the projection of a small part of the inner surface of the colon onto the cylinder. This avoids the appearance of double polyps since intersections can only appear between different frames. However, this approach does not provide a complete overview of the colon. They have presented

*Email: {weihong|gu|qfeng|mjin|ari}@cs.sunysb.edu

a new two step technique to deal with double appearance of the polyps and nonuniform sampling problems [Bartrolí et al. 2001a]. First, curved rays are cast along the negative gradient of the distance map from the central path of the colon, which return the distance between the camera and the intersection points on the colon surface. Then, the height field is unfolded and the nonlinear 2D scaling is applied to achieve area preservation. However, it is important to this method that the central path is smooth and has as many linear segments as possible.

Haker et al. [2000] have proposed a method based on the discretization of the Laplace-Beltrami operator to flatten the colon surface onto the plane in a manner which preserves angles. The flattened colon surface is colored according to its mean curvature. A morphological method is used to remove minute handles resulting from the segmentation algorithm, because their algorithm requires the input surface to be a topologically open-ended cylinder. However, the color-coded mean curvature of the extracted surface is not efficient for polyp identification, and it requires a highly accurate and smooth surface mesh to achieve a good mean-curvature calculation. Furthermore, our method maps the colon surface to a planar rectangle, while their method maps the colon surface to a planar parallelogram.

We propose a novel method for colon flattening by computing the conformal structure of the surface, represented as a set of holomorphic 1-form basis. It has the following advantages: 1)The algorithm is rigorous and theoretically solid, which is based on the Riemann surface theory and differential geometry; 2)It is general, so it can handle high genus surfaces; 3)The global distortion from the colon surface to the parametric rectangle is minimized, which is measured by harmonic energy; 4)It is angle preserving, so the shape of the polyps is preserved; 5)The topology noise is removed automatically by our shortest loop algorithm. Combined with the direct volume rendering method, the flattened 2D colon image provides an efficient way to enhance virtual colonoscopy systems.

The remainder of this paper is organized as follows. The shortest loop algorithm for topological denoising is presented in Section 2. The algorithm to flatten the colon surface with conformal mapping is discussed in Section 3. The direct volume rendering algorithm for the flattened colon surface is described in Section 4. The implementation and experiment results are reported in Section 5. In Section 6, concluding remarks are drawn, and future work of this subject is summarized.

2 Topological Denoising

The colon surfaces reconstructed from CT dataset usually have complicated topologies caused by the noise and inaccuracy of the reconstruction methods. In general several spurious handles will be introduced to a surface. This topological noise complicates our flattening algorithm, and introduces large distortions.

It is challenging to locate these handles and remove them using special "topology surgery". El-sana and Varshney [1997] have proposed a topology controlled simplification method for polygonal models. Tiny tunnels are identified by rolling a sphere of small radius over the object. Guskov and Wood [2001] have presented a local wave front traversal algorithm to discover the local topologies of the mesh and identify features such as small tunnels. The mesh is then cut and sealed along non-separating cuts, reducing the topological complexity of the mesh. These methods are efficient for tiny handle identification. However, we find that handles are not tiny in our colon data sets as shown in Figure 2. Our approach is different in that it identifies handles by locating the shortest loop for each homotopy class.

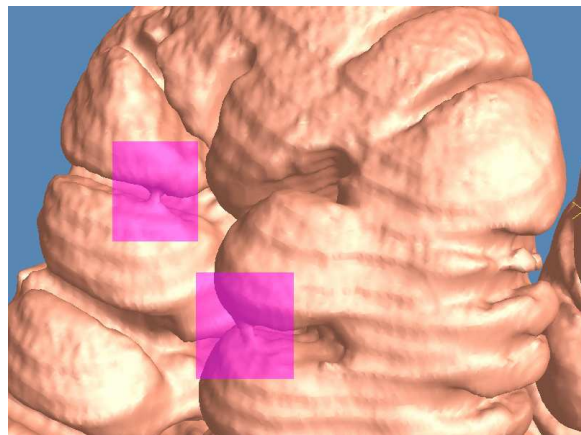


Figure 2: A zoomed view of a colon surface with two handles.

2.1 Handle Identification

Intuitively, the topology of a closed oriented surface is determined by the number of handles (genus). Two closed curves are *homotopic* if they can deform to each other on the surface. Homotopic equivalence classes form the so-called *homotopy* group, which has finite generators, i.e. *homology basis*. Each handle corresponds to two generators. A handle can be removed by cutting the handle along one of its generators, and filling the resulting holes as shown in Figure 3.

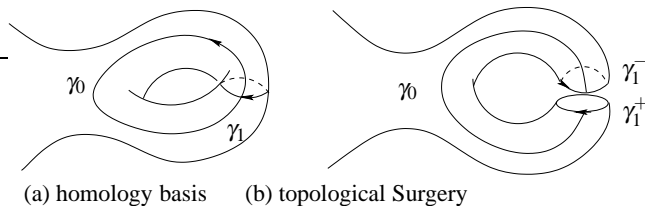


Figure 3: Homology basis and topological surgery.

It is highly desirable to locate the shortest (or optimal) loop in each *homotopy* group [Éric Colin de Verdière and Lazarus 2005]. This requires the techniques of *covering space*. Suppose that \tilde{M} and M are two surfaces, then (\tilde{M}, π) is said to be a covering space of M if $\pi : \tilde{M} \rightarrow M$ is a surjective continuous map with every $p \in M$ having an open neighborhood U such that every connected component $\pi^{-1}(U)$ is mapped homeomorphically onto U by π . If \tilde{M} is simply connected, then it is said a *universal covering space* of M . A simply connected region $\tilde{M} \subset \tilde{M}$ is called a *fundamental domain*, if the restriction of π on \tilde{M} is bijective. Intuitively, one can slice M along some curve set (cut graph) to obtain a topological disk (a fundamental domain), and glue fundamental domains coherently to form the universal covering space.

For any point $p \in M$, its preimages are the discrete set $\pi^{-1}(p) = \{\tilde{p}_0, \tilde{p}_1, \tilde{p}_2, \tilde{p}_3, \dots\} \subset \tilde{M}$. If $\tilde{\gamma}_k$ is a curve connecting \tilde{p}_0 and \tilde{p}_k in the universal covering space \tilde{M} , then $\gamma_k = \pi(\tilde{\gamma}_k)$ is a closed loop on M . By going through all end points \tilde{p}_k , γ_k goes through all homotopy classes. In order to find the shortest loop γ_k in each homotopy class, we can find the shortest path $\tilde{\gamma}_k$ in the universal covering space instead. Figure 4 demonstrates the concepts of fundamental domain and universal covering space using a genus one surface. It illustrates the idea of lifting a loop to a path and converting the shortest loop problem to the shortest path problem.

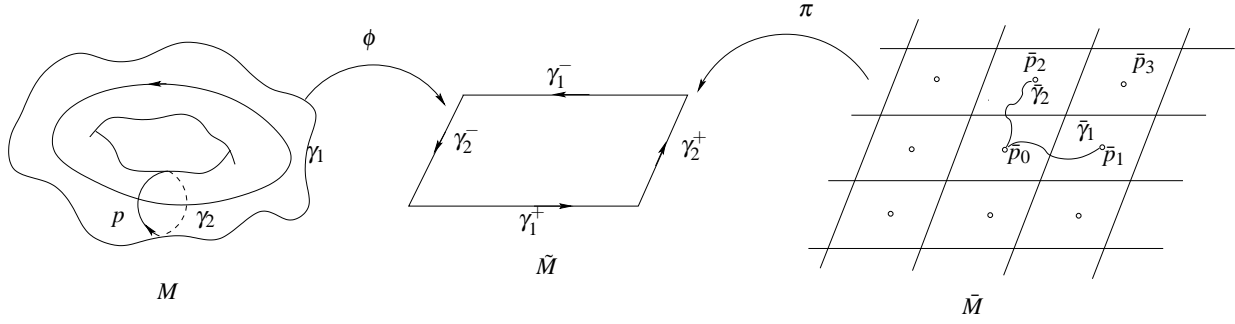


Figure 4: Topology Concepts: Two curves γ_1, γ_2 on a surface M form a *cut graph*. M is sliced open along the cut graph to become a *fundamental domain* \tilde{M} , γ_i is mapped to γ_i^+ and γ_i^- . By gluing many copies of \tilde{M} such that γ_i^+ is glued with γ_i^- , the *universal covering space* \bar{M} can be obtained. $\pi: \bar{M} \rightarrow M$ is the projection map. Any point p on M has a discrete preimage set $\pi^{-1}(p) = \{\bar{p}_0, \bar{p}_1, \bar{p}_2, \dots\}$. Any closed curves through p on M are lifted as curve segments connecting two points in $\pi^{-1}(p)$, e.g. γ_1 is lifted as $\tilde{\gamma}_1$, γ_2 is lifted as $\tilde{\gamma}_2$. The shortest loops on M correspond to the shortest path on \bar{M} .

2.2 Denoising Algorithm

Given a closed mesh M , we want to compute its cut graph Γ , its homology basis, its fundamental domain \tilde{M} , and find the shortest loop homotopic to the base loops. In the following discussion, we assume the surfaces are represented by meshes using the halfedge data structure. We use f to denote a face, e for a halfedge, e^- for the dual halfedge of e , M for mesh, \tilde{M} for the fundamental domain of M , \bar{M} for the universal covering space of M .

2.2.1 Computing Cut Graph and Homology Basis

The algorithm to compute the *cut graph* and *homology basis* for a genus g surface M is as follows:

1. Arbitrarily select a seed face $f_1 \in M$, let $M \leftarrow M/f_1$, and $\tilde{M} \leftarrow f_1$. Suppose $\partial f_1 = e_1 e_2 e_3$, then $\partial \tilde{M} = e_1 e_2 e_3$.
2. Suppose at current stage

$$\partial \tilde{M} = e_1 e_2, \dots, e_n$$

Choose a halfedge e_k from the boundary of \tilde{M} . Suppose e_k^- is associated with a face $f \in M$, $\partial f = e_k^- \tau_1 \tau_2$, then glue f with \tilde{M} by identifying $e_k^- \in \partial f$ and $e_k \in \partial \tilde{M}$, let $\tilde{M} \leftarrow \tilde{M} \cup_{e_k} f$ and $M \leftarrow M/f$. Update the boundaries

$$\partial \tilde{M} = e_1 e_2, \dots, e_{k-1}, \tau_1, \tau_2, e_{k+1}, \dots, e_n$$

3. Repeat step 2, until $M = \emptyset$. The faces are removed from M one by one, the first one is denoted as f_1 , the second one is f_2 and so on.
4. $\partial \tilde{M}$ is a loop composed by a sequence of halfedges, then all the edges whose halfedges are in $\partial \tilde{M}$ form the cut graph Γ .
5. Compute a spanning tree T of graph Γ . Suppose

$$\Gamma - T = \{e_1, e_2, \dots, e_{2g}\},$$

where e_i are edges. Then $T \cup e_k$ has a unique loop γ_k . The set of the loops $\{\gamma_1, \gamma_2, \dots, \gamma_{2g}\}$ forms a homology basis of M .

2.2.2 Computing Fundamental Domain

First we simplify the cut graph Γ , then slice M along the simplified cut graph to form the fundamental domain \tilde{M} . The algorithm to construct a fundamental domain is as follows:

1. Compute the valence of each vertex $v \in \Gamma$, which is the number of edges connecting with v . All vertices with valence other than 2 are called nodes. The nodes segment Γ to segments.
2. Repeat removing all segments attached to valence 1 nodes, until all nodes in Γ have valence more than 2.
3. Slice M along the simplified cut graph to get a fundamental domain \tilde{M} . $\partial \tilde{M} = s_1 s_2 s_2 \dots s_n$, where s_k is a segment in Γ .

2.2.3 Constructing a Finite Portion of Universal Covering Space

By gluing finite copies of the fundamental domain \tilde{M} coherently, a finite portion of the universal covering space can be constructed.

1. Set $\bar{M} \leftarrow \tilde{M}$, $\partial \bar{M} = \partial \tilde{M} = \tau_1 \tau_2 \dots \tau_m$.
2. Suppose at current stage, the boundary of \bar{M} is

$$\partial \bar{M} = s_1 s_2 \dots s_n.$$

Select a segment $s_k \in \partial \bar{M}$, then find $\tau_j^- \in \partial \tilde{M}$ such that $s_k = \tau_j^-$, and glue \bar{M} with \tilde{M} by identifying $s_k \in \partial \bar{M}$ with $\tau_j^- \in \partial \tilde{M}$. Update the boundary of \bar{M}

$$\partial \bar{M} = s_1 s_2 \dots s_{k-1} \tau_{j+1} \tau_{j+2} \dots \tau_m \tau_1 \tau_2 \dots \tau_{j-1} s_{k+1} \dots s_n.$$

3. Go through the segment list of $\partial \bar{M}$, if $s_k s_{k+1} \subset \partial \bar{M}$ and $s_k = s_{k+1}^-$, then merge s_k and s_{k+1} on \bar{M} . Repeat this process, until there is no such kind of adjacent dual pair.
4. Repeat step 2 and 3 several times to get a finite portion of the universal covering space. During the gluing, each copy of the fundamental domain has a unique identifier k , and denoted as \tilde{M}_k .

Each vertex in $\bar{v} \in \bar{M}$ corresponds to a unique vertex $v \in M$, this map is the projection map π , the correspondences between edges and faces are induced by π naturally.

2.2.4 Computing Shortest Loop

Verdière et al. [2005] presented an algorithm to compute a shortest loop, which has polynomial running time if the lengths of the edges are uniform. They prove that the result of their algorithm is a shortest loop among all simple loops in its homotopy class. In this algorithm, each closed curve on M can be lifted as a path in the universal covering space \bar{M} . The shortest loop in each homotopy group can be computed by finding the shortest path in the universal covering space.

2.2.5 Noise Removing

After computing a homology basis $\{\gamma_1, \gamma_2, \dots, \gamma_g\}$ of M , its shortest homology basis $\{\gamma'_1, \gamma'_2, \dots, \gamma'_g\}$ can be computed using the above algorithms. Each handle of M corresponds to two loops. A topology noise (i.e. minute handle) has a loop with very small length. Topology noise is removed by using the following algorithm:

1. Compute the shortest homology basis $\{\gamma'_1, \gamma'_2, \dots, \gamma'_g\}$ of M .
2. Select γ' from the basis with the minimal length.
3. Slice M along γ , to get two boundary curves γ^+ and γ^- .
4. Fill γ^+ by a polygon, fill γ^- by a polygon, triangulate the filled mesh to get the resulting mesh \bar{M} .
5. Repeat 2 through 4, until no minute handles are left.

3 Conformal Flattening

In our method, the colon surface is conformally mapped to a planar rectangle. Because conformal maps have special properties, which are extremely valuable for real applications:

- Conformal maps are *angle preserving (local shape preserving)*. Because analytic functions are angle preserving, therefore by definition, conformal maps preserve angles. For example, any two intersecting curves γ_1 and γ_2 are mapped to $f(\gamma_1)$ on M_2 and $f(\gamma_2)$ by a conformal map f , then the intersection angle between γ_1 and γ_2 equals to the intersection angle between $f(\gamma_1)$ and $f(\gamma_2)$. Polyps still can be identified based on their shape on the flattened colon image.
- Conformal maps minimize elastic energy (*harmonic energy*). One can treat M_1 as a rubber surface, the mapping to another surface will introduce stretching distortion and generate the elastic energy. It has been proven [Jost 2002] that conformal maps minimize the harmonic energy. It is highly desirable in practice to find the best match between two surfaces which minimize the distortion.
- Conformal maps are *intrinsic*. Conformal maps are determined by the metric, not the embedding. For example, one can change a surface by rotation, translation, folding, bending without stretching, the conformal parameterization is invariant. This is valuable for surface registration purpose.
- Conformal maps are *stable* and easy to compute. Computing conformal maps is equivalent to solve an elliptic geometric PDE [Schoen and Yau 1997], which are stable and insensitive

to the noise and the resolution of the data. If two surfaces are similar to each other, then the corresponding conformal maps are similar also.

- Conformal parameterization simplifies geometric processing from 3D to 2D. By parameterizing a surface, we map it to the planar domain with local shape preservation. Some of the 3D geometric features are carried by the mapping with high fidelity. For example, figure 9 illustrates the polyp on a colon surface both in 3D and in the conformal parameter domain. It is obvious that the shape of the polyp is well preserved on the plane. It is easier to process in the planar domain than in the 3D domain. Furthermore, many differential operators (such as the Laplace-Beltrami operator) are in the simplest form under conformal parameterization.

In the following sections, we first briefly introduce the major concepts and theorems used in our colon flattening algorithms. Thorough discussion can be found in Riemann surface theory [Jost 2002]. Then, the detail of the flattening algorithm will be presented.

3.1 Riemann Surface Theory

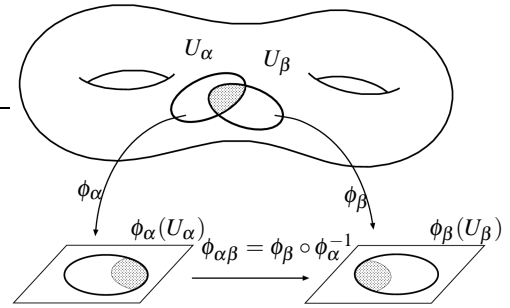


Figure 5: Riemann Surface: The manifold is covered by a set of charts (U_α, ϕ_α) , where $\phi_\alpha : U_\alpha \rightarrow \mathbf{R}^2$. If two charts (U_α, ϕ_α) and (U_β, ϕ_β) overlap, the transition function $\phi_{\alpha\beta} : \mathbf{R}^2 \rightarrow \mathbf{R}^2$ is defined as $\phi_{\alpha\beta} = \phi_\beta \circ \phi_\alpha^{-1}$. If all transition functions are analytic, then the manifold is a Riemann surface. The atlas $\{(U_\alpha, \phi_\alpha)\}$ is a conformal structure.

A manifold can be treated as a set of open sets in \mathbf{R}^2 glued coherently.

Definition 3.1 A 2-dimensional manifold is a connected Hausdorff space M for which every point has a neighborhood U that is homeomorphic to an open set V of \mathbf{R}^2 . Such a homeomorphism $\phi : U \rightarrow V$ is called a coordinate chart. An atlas is a family of charts $\{(U_\alpha, \phi_\alpha)\}$, where U_α constitutes an open covering of M .

Definition 3.2 (Analytic Function) A complex function $f : \mathbf{C} \rightarrow \mathbf{C}$, $(x, y) \rightarrow (u, v)$ is analytic (holomorphic), if it satisfies the following Riemann-Cauchy equation

$$\frac{\partial u}{\partial x} = \frac{\partial v}{\partial y}, \quad \frac{\partial u}{\partial y} = -\frac{\partial v}{\partial x}.$$

A conformal atlas is an atlas with special transition functions.

Definition 3.3 (Riemann Surface) Suppose M is a 2-dimensional manifold with an atlas $\{(U_\alpha, \phi_\alpha)\}$. If all chart transition functions

$$\phi_{\alpha\beta} := \phi_\beta \circ \phi_\alpha^{-1} : \phi_\alpha(U_\alpha \cap U_\beta) \rightarrow \phi_\beta(U_\alpha \cap U_\beta)$$

are analytic, then the atlas is called a conformal atlas, and M is called a Riemann surface.

Two conformal atlases are *compatible* if their union is still a conformal atlas. All the compatible conformal atlases form a *conformal structure* of the manifold as shown in Figure 5. All oriented 2-dimensional manifolds with Riemannian metrics are Riemann surfaces and have conformal structures [Jost 2002], such that on each chart (U_α, ϕ_α) with local parameter (u, v) , the metric can be represented as $ds^2 = \lambda(u, v)(du^2 + dv^2)$.

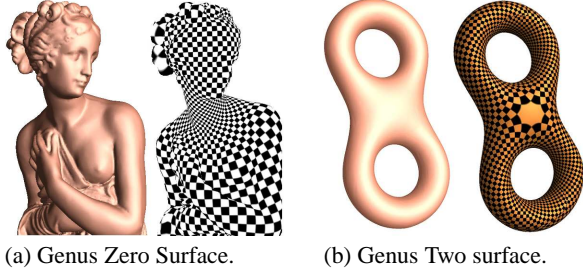


Figure 6: Holomorphic 1-form examples for genus zero and genus two surfaces.

3.1.1 Holomorphic 1-form

In order to flatten the surface, we need special differential forms defined on the conformal structure.

Definition 3.4 (Holomorphic 1-form) *Given a Riemann surface M with a conformal structure \mathcal{A} , a holomorphic 1-form ω is a complex differential form, such that on each local chart $(U, \phi) \in \mathcal{A}$,*

$$\omega = f(z)dz,$$

where $f(z)$ is an analytic function, $z = u + iv$ is the local parameter in the complex form.

The holomorphic 1-forms of closed genus g surface form a g complex dimensional linear space, denoted as $\Omega(M)$. It is noted that a genus zero surface has no holomorphic 1-forms. A conformal atlas can be constructed by using a basis of $\Omega(M)$. Considering its geometric intuition, a holomorphic 1-form can be visualized as two vector fields $\omega = (\omega_x, \omega_y)$, such that the curls of ω_x and ω_y equal zero. Furthermore, one can rotate ω_x about the normal a right angle to arrive at ω_y ,

$$\nabla \times \omega_x = 0, \nabla \times \omega_y = 0, \omega_y = n \times \omega_x.$$

3.1.2 Conformal Parameterization

Suppose $\{\omega_1, \omega_2, \dots, \omega_g\}$ is a basis for $\Omega(M)$, where g is genus of M . We can find a collection of open disks $U_\alpha \subset M$, such that U_α form an open covering of M , $M \subset \cup U_\alpha$. We define $\phi_\alpha^k : U_\alpha \rightarrow \mathbf{C}$ using the following formula, first we fix a base point $p \in U_\alpha$, for any point $q \in U_\alpha$,

$$\phi_\alpha^k(q) = \int_\gamma \omega_k,$$

where the path $\gamma : [0, 1] \rightarrow U_\alpha$ is arbitrary curve connecting p and q and inside U_α , $\gamma \subset U_\alpha$, $\gamma(0) = p$, $\gamma(1) = q$. It can be verified that, we can select a $\phi_\alpha^k, k = 1, 2, \dots, g$, such that ϕ_α^k is a bijection, we simply denote it as ϕ_α . Then the atlas $\{(U_\alpha, \phi_\alpha^k)\}$ is a conformal atlas.

For a genus one closed surface M , given a holomorphic 1-form $\omega \in \Omega(M)$, we can find 2 special curves $\Gamma = \gamma_1 \cup \gamma_2$, such that $\tilde{M} = M/\Gamma$ is a topological disk. Furthermore, on each open set U_α , if the curve $\int_{\gamma_1} \omega$ is a horizontal line in the parameter plane, then γ_1

is a *horizontal trajectory*. In the current work, we choose γ_2 such that $\int_{\gamma_2} \omega$ is a vertical line in the parameter plane, namely, γ_2 is a vertical trajectory. Γ is called a *cut graph*.

Then by integrating ω on \tilde{M} , \tilde{M} is conformally mapped to a parallelogram, as shown in figure 4. Figure 6 illustrates holomorphic 1-forms on surfaces. The texture coordinates are obtained by integrating the 1-form on the surface.

3.1.3 Conformal Maps

Suppose M_1 is a Riemann surface with a conformal atlas $\{(U_\alpha, \phi_\alpha)\}$, and M_2 is another Riemann surface with conformal atlas $\{(V_\beta, \tau_\beta)\}$.

Definition 3.5 (Conformal Map) *A map $f : M_1 \rightarrow M_2$ is a conformal map, if its restriction on any local charts (U_α, ϕ_α) and (V_β, τ_β) ,*

$$f_\alpha^\beta := \tau_\beta \circ f \circ \phi_\alpha^{-1} : \phi_\alpha(U_\alpha) \rightarrow \tau_\beta(V_\beta)$$

is analytic.

3.2 Flattening Algorithm

The concepts of Riemann surface and conformal map are defined using continuous mathematics. Computing conformal parameterization is equivalent to solving an elliptic partial differential equation on surfaces.

Unfortunately, in reality, all surfaces are represented by discrete piecewise linear meshes, which are not differentiable in general. Fortunately, the solution to the elliptic PDE can be approximated accurately by piecewise linear functions using finite element method [Reddy 2004]. The convergence and accuracy have been thoroughly analyzed in finite element field.

Therefore, our algorithm is mainly based on the finite element method. The key step is to use piecewise linear functions defined on edges to approximate differential forms. Furthermore, the forms minimize the harmonic energy, the existence and the uniqueness are guaranteed by Hodge theory [Schoen and Yau 1997].

3.2.1 Double Covering

In our case, after the topological noise removal, the surface is a closed genus zero surface. Because the genus zero surface has no holomorphic 1-form, a *double covering* method is used to construct a genus one surface. Two holes are first punched on the input surface. Then, a mesh M with two boundaries is obtained. The algorithm to construct a closed genus one mesh is described as follows:

1. Make a copy of mesh M , denoted as M' , such that M' has all vertices in M , if $[v_0, v_1, v_2]$ is a face in M , then $[v_1, v_0, v_2]$ is a face of M' .
2. Glue M and M' along their boundaries, if a halfedge $[v_0, v_1]$ is on the boundary of M $[v_0, v_1] \in \partial M$, then $[v_1, v_0]$ is on the boundary of M' . Glue $[v_0, v_1]$ with $[v_1, v_0]$.

The resulting mesh is a closed and symmetric, with two layers coincided. It is noted that general genus one surface can be conformally mapped to a planar parallelogram, but not a rectangle. In our case, the genus one surface is obtained by double covering method. The Riemann metric defined on the double covered surface is symmetric. Each boundary where we glue two surfaces is mapped to a straight line. Thus, the denoised genus zero colon surface can be conformally mapped to a rectangle.

3.2.2 Computing Harmonic and Holomorphic 1-form

After getting the homology basis $\{\gamma_1, \gamma_2, \dots, \gamma_g\}$, it is easy to compute the holomorphic 1-form basis.

1. Select γ_k , compute $\omega_k : K_1 \rightarrow \mathbf{R}$, form the boundary condition:

$$\sum_{e \in \gamma_i} \omega_k(e) = \delta_i^k, \omega_k(\partial f) = 0, \forall f \in K_2, \quad (1)$$

where

$$\delta_i^k = \begin{cases} 1 & : i = k \\ 0 & : i \neq k \end{cases}$$

K_1 is the edge set of M and K_2 is the face set of M .

2. Under above linear constraints, compute ω_k minimizing the quadratic energy,

$$E(\omega_k) = \sum_{e \in K_1} k_e \omega_k^2(e), \quad (2)$$

using linear constrained least square method, where k_e is the weight associated with each edge, suppose the angles in the adjacent faces against edge e are α, β , then $k_e = \frac{1}{2}(\cot \alpha + \cot \beta)$ [Pinkall and Polthier 1993]. Solving this equation is equivalent to solve Riemann-Cauchy equation using finite element method.

3. On face $[v_0, v_1, v_2]$, its normal n is computed first, and a unique vector v in the same plane of v_0, v_1, v_2 is obtained by solving following equations:

$$\begin{cases} \langle v_1 - v_0, v \rangle = \omega_k([v_1, v_0]) \\ \langle v_2 - v_1, v \rangle = \omega_k([v_2, v_1]) \\ \langle n, v \rangle = 0 \end{cases} \quad (3)$$

Rotate v about n a right angle, $v^* = n \times v$, then define

$$\omega_k^*([v_i, v_j]) := \langle v_j - v_i, v^* \rangle.$$

The harmonic 1-form basis is represented by $\{\omega_1, \omega_2, \dots, \omega_{2g}\}$, and the holomorphic 1-form basis is given by $\{\omega_1 + i\omega_1^*, \omega_2 + i\omega_2^*, \dots, \omega_{2g} + i\omega_{2g}^*\}$.

3.2.3 Conformal Parameterization

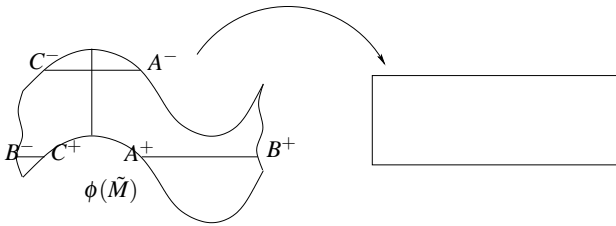


Figure 7: Trace horizontal trajectory.

Suppose we have selected a holomorphic 1-form $\omega : K_1 \rightarrow \mathbf{C}$, then we define a map $\phi : \tilde{M} \rightarrow \mathbf{C}$ by integration. The algorithm to trace the horizontal trajectory and the vertical trajectory on $\phi(\tilde{M})$ is as follows:

1. Pick one vertex $p \in \tilde{M}$ as the base vertex.
2. For any vertex $q \in \tilde{M}$, find the shortest path $\gamma \in D$ connecting p to q .

3. Map q to the complex plane by

$$\phi(q) = \sum_{e \in \gamma} \omega(e).$$

4. Pick a vertex $p \in M$, trace the horizontal line γ on the plane region $\phi(\tilde{M})$ through $\phi(p)$. If γ hits the boundary of $\phi(\tilde{M})$ at the point $\phi(q)$, q must be in the cut graph Γ , then there are two points q^+, q^- on the boundary of \tilde{M} , $\partial\tilde{M}$. Assume γ hits $\phi(q^+)$, then we continue to trace the horizontal line started from $\phi(q^-)$, until we return to the starting point $\phi(p)$. The horizontal trajectory is $\phi^{-1}(\gamma)$.
5. Trace vertical trajectory similar to step 4.
6. The new cut graph $\tilde{\Gamma}$ is the union of the horizontal and vertical trajectories. Cut the surface along $\tilde{\Gamma}$ to get \tilde{M}' , and compute $\tilde{\phi}$. Then $\tilde{\phi}(\tilde{M}')$ is a rectangle, $\tilde{\phi}$ is a conformal map.

4 Direct Volume Rendering

The result of the flattening algorithm is a triangulated rectangle where the polyps are also flattened. The rendering of the flattened colon image is crucial for the detection of polyps. Haker et al. [2000] use color-coded mean curvature to visualize the flattened colon surface. Although it can show the geometry information of the 3D colon surface, it is still unnatural for the physicians to detect the polyps. The shape of the polyps is a good clue for polyp detection. In this section, we describe a direct volume rendering method to render the flattened image. Each pixel of the flattened image is shaded using a fragment program executed on the GPU, which allows the physician to move and zoom a viewing window to inspect the entire flattened inner colon surface. The idea of our rendering algorithm is to map each pixel of the flattened image back to the 3D colon surface, i.e., the volume space. The pixel is shaded using volumetric ray-casting algorithm in the volume space.

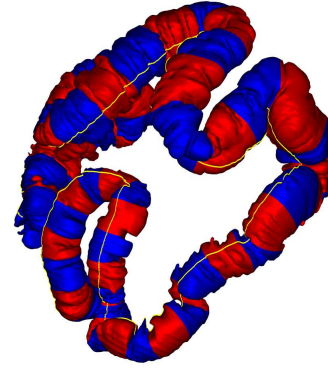


Figure 8: The colon is divided into N segments.

4.1 Camera Registration

In order to perform the ray-casting algorithm, the ray direction needs to be determined for each vertex of the 3D colon surface first. A number of cameras are uniformly placed on the central path of the colon. The ray direction of a vertex is then determined by the nearest camera to that vertex.

Our camera registration algorithm starts with approximating the central path with a B-spline and resampling it into uniform intervals. Each sampling point represents a camera. Each vertex is then

registered with a sampling point on the central path. The registration procedure is implemented efficiently by first dividing the 3D colon surface and central path into N segments. The registration is then performed between the correspondent segments of colon and the central path. The division of the 3D colon is done by classifying the vertices of the flattened 2D mesh into uniform N segments based on their height. As a consequence, the vertices of the 3D colon mesh are also divided into N segments, as shown in Figure 8. We then trace $N - 1$ horizontal lines on the flattened 2D mesh, which uniformly divide the 2D mesh into N segments. Each traced horizontal line corresponds to a cross contour on the 3D mesh. In fact, we do not need to really trace the horizontal lines. For each horizontal line, we only need to compute the intersection points of the horizontal line and edges intersecting with it. For each intersection point, the corresponding 3D vertex of the 3D colon mesh is then interpolated. The centroid of these interpolated 3D vertices is computed and registered with a sampling point of the central path. Therefore, the central path is also divided into N segments, and each segment of the 3D colon mesh corresponds to a segment of the central path. Although the division of the 3D colon surface and the central path is not uniform as that of the 2D mesh, it does not affect the accuracy of the camera registration.

For each vertex of a colon surface segment, we find its nearest sampling point in its corresponding central path segment and the neighboring two segments. This algorithm is efficient because for each vertex the comparison is performed only with a small number of sampling points on the central path. For each vertex, we only record the B-spline index of the sampling points, instead of its 3D coordinates.

4.2 Volumetric Ray-Casting

To generate a high-quality image of the flattened colon, only coloring the vertices of the polygonal mesh and applying linear interpolation is not sufficient. We need to determine the color for each pixel of the 2D image. This can be performed efficiently using a fragment program on the GPU. For each vertex of the flattened polygonal mesh, we pass its corresponding 3D coordinates and camera index through texture coordinates to the fragment program. When the flattened polygonal mesh is rendered, each pixel of the flattened image will obtain its barycentric interpolated 3D coordinates and camera index. Its 3D position may not be exactly on the colon surface, but very close to the colon surface. Because we use a direct volume rendering method to determine the color for the pixel, it does not affect the image quality. We use the interpolated camera index to look up its correspondent sampling point on the central path. Then, the ray direction is determined and volumetric ray casting algorithm is performed using an opaque transfer function. By this method, we can determine the color for each pixel on the flattened image to generate a high-quality image.

Since our flattened image is colored per-pixel, we can provide the physician with a high-quality zoom-in view of a suspicious area on the flattened image in real-time. Because each vertex is registered with a sampling point on the central path, the flattened colon image can be easily correlated with the navigation of a virtual colonoscopy system. The correlated 3D view of the suspicious area can be also shown simultaneously.

5 Implementation and Results

We have implemented our conformal flattening and rendering algorithm in C/C++ and run all the experiments on a uni-processor 3.0 GHz Pentium IV PC running Windows XP, with 2G RAM and NVIDIA Geforce 6800GT graphics board. A large number of colon CT data sets have been used to test our algorithms. All data sets

have a large number of slices (> 350), and the resolution of each slice is 512×512 . They all exhibit similar results.

5.1 Preprocessing

Before our colon flattening algorithm can be applied, we need to perform the following tasks to extract the colon surface from the CT data set. First, a segmentation algorithm [Lakare et al. 2000] is applied, and a binary mask is generated, which labels the voxels belonging to the colon interior and the colon wall. This algorithm ensures a fast and accurate segmentation with the ability to remove the partial volume effect. Second, the rendering algorithm involves the central path of the colon. The central path is automatically extracted from the CT data set based on an accurate DFB-distance field with the exact Euclidian values [Wan et al. 2002]. The path is then approximated by a B-spline curve. Finally, given the binary mask and the CT data set, an enhanced dual contouring method [Zhang et al. 2004] is used to extract the simplified colon surface while preserving the finest resolution isosurface topology. Since our algorithm can deal with small handles, we do not need to remove these handles in the preprocessing step. All these algorithms used in the preprocessing step are robust and efficient, and can be done in seconds on the PC platform.

5.2 Discussion

One of the CT colon datasets that we use has the resolution of $512 \times 512 \times 460$ and contains two polyps. The size of one polyp is 8×9 mm, and the size of the other polyp is 3×4 mm. Five minute handles are removed from the colon surface automatically, before applying the flattening algorithm. A flattened image of the whole colon using our rendering algorithm is shown in Figure 10. The resolution of the flatted image is 196×4000 , and it is shown in three separate pictures. The rendering time for this image is about 300ms. The larger polyp can be inspected from Figure 10(a), which is surrounded by a circle. However, the smaller polyp located in Figure 10(c) is hard to recognize. Therefore, in a real medical application, the resolution should be at least four times higher than the one we used in this paper. In fact, we do not need to pre-compute such a high resolution flattened image. Our rendering algorithm with the acceleration of the commodity graphics hardware can provide a real-time high-quality zoom-in function, which allows the physician to interactively inspect the entire flattened colon.

In Figure 9(a), we show the larger polyp rendered using the volumetric ray-casting algorithm by positioning a camera in front of the polyp. In Figure 9(b), we show a zoom-in view generated by our rendering algorithm showing the same polyp. We can clearly see that our flattening algorithm well preserves the shape of the polyp. In Figure 9(c) and 9(d), we show a 3D fly-through image and a zoom-in flattened image, respectively. The smaller polyp can be clearly recognized in the zoom-in image.

The whole process of the presented algorithm can be completed in about 30 minutes. Most steps of our algorithm are done within seconds or minutes. The most time consuming part of our algorithm is computing the harmonic holomorphic 1-form using the conjugate gradient method, which takes about several minutes. The good thing is that the conjugate gradient method can be accelerated with the GPU [Bolz et al. 2003].

6 Conclusions

We have presented an efficient colon flattening algorithm using conformal structure. Our algorithm is general for all high genus surfaces, and does not require the input surface to be a topological cylinder. The topology noise (i.e., minute handle) is removed automatically by our shortest loop algorithm. We have proven that our

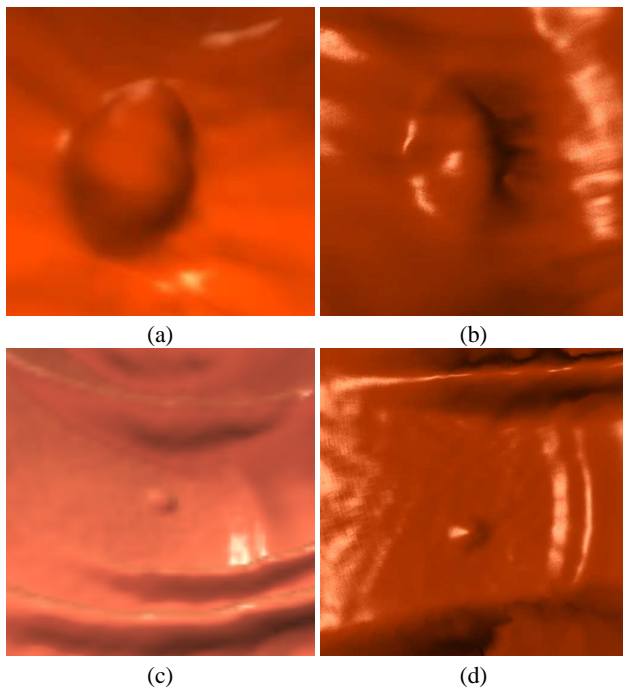


Figure 9: (a) A close view of a polyp rendered with the volumetric ray casting, (b) A view generated from the flattened colon image showing the same polyp. (c) A view contains a small polyp generated from the navigation of a virtual colonoscopy system. (d) A view generated from the flattened colon image.

algorithm is angle preserving and the global distortion is minimal. The shape of the polyps on the flattened colon image is well preserved, and can be easily identified by a physician. The flattened colon image is rendered with a direct volume rendering method accelerated with commodity graphics hardware. We demonstrate that the conformal colon flattening image cooperates well with the fly-through virtual colonoscopy system.

We have some on-going research work. Since our flattening algorithm is not limited to a genus one surface, we are in the process of applying our algorithm to other human organs, such as the heart. The polyp is well shown in the flattened 2D image. We are experimenting with clustering algorithms and pattern recognizing techniques to detect polyps automatically on the flattened colon image.

Acknowledgement

This work has been partially supported by NSF grant CCR-0306438, NSF CAREER grant CCF-0448339, and NIH grants CA79180 and CA110186. The CT colon datasets are courtesy of Stony Brook University Hospital. AK discloses that he owns a fraction of Viatronix shares.

References

BALOGH, E., SORANTIN, E., NYUL, L. G., PALAGYI, K., KUBA, A., WERKGARTNER, G., AND SPULLER, E. 2002. Colon unraveling based on electronic field: Recent progress and future work. *Proceedings SPIE 4681*, 713–721.

BARTROLÍ, A. V., WEGENKITTL, R., KÖNIG, A., AND GRÖLLER, E. 2001. Nonlinear virtual colon unfolding. In *IEEE Visualization '01*, 411–418.

BARTROLÍ, A. V., WEGENKITTL, R., KÖNIG, A., GRÖLLER, E., AND SORANTIN, E. 2001. Virtual colon flattening. *VisSym Joint Eurographics - IEEE TCVG Symposium on Visualization*, 127–136.

BOLZ, J., FARMER, I., GRINSPUN, E., AND SCHRÖDER, P. 2003. Sparse matrix solvers on the gpu: Conjugate gradients and multi-grid. *ACM Transactions on Graphics* 22, 3, 917–924.

CORMEN, T. H., LEISERSON, C. E., RIVEST, R. L., AND STEIN, C. 2001. *Introduction to Algorithms, Second Edition*. The MIT Press.

EI-SANA, J., AND VARSHNEY, A. 1997. Controlled simplification of genus for polygonal models. *IEEE Visualization*, 403–412.

ÉRIC COLIN DE VERDIÈRE, AND LAZARUS, F. 2005. Optimal system of loops on an orientable surface. *Discrete and Computational Geometry* 33, 3, 507–534.

ERICKSON, J., AND WHITTLESEY, K. 2005. Greedy optimal homotopy and homology generators. *ACM-SIAM Symposium on Discrete Algorithms*, 1038–1046.

GUSKOV, I., AND WOOD, Z. 2001. Topological noise removal. *Graphics Interface 2001*, 19–26.

HAKER, S., ANGENENT, S., TANNENBAUM, A., AND KIKINIS, R. 2000. Nondistorting flattening maps and the 3d visualization of colon ct images. *IEEE Transactions on Medical Imaging* 19, 7, 665–670.

HONG, L., MURAKI, S., KAUFMAN, A., BARTZ, D., AND HE, T. 1997. Virtual voyage: Interactive navigation in the human colon. In *Proceedings of ACM SIGGRAPH 1997*, 27–34.

JOST, J. 2002. *Compact Riemann Surfaces*. Springer.

LAKARE, S., WAN, M., SATO, M., AND KAUFMAN, A. 2000. 3d digital cleansing using segmentation rays. In *IEEE Visualization '00*, 37–44.

MASSEY, W. S. 1990. *Algebraic Topology: An Introduction*. Springer.

PAIK, D. S., BEAULIEU, C. F., JEFFREY, R. B. J., KARADI, C. A., AND NAPEL, S. 2000. Visualization modes for ct colonography using cylindrical and planar map projections. *Journal of Computer Assisted Tomography* 24, 179–188.

PINKALL, U., AND POLTHIER, K. 1993. Computing discrete minimal surfaces and their conjugates. *Experimental Mathematics* 2, 1, 15–36.

REDDY, J. N. 2004. *An Introduction to Nonlinear Finite Element Analysis*. Oxford University Press.

SCHOEN, R., AND YAU, S.-T. 1997. *Lectures on Harmonic Maps*. International Press.

WAN, M., LIANG, Z., KE, Q., HONG, L., BITTER, I., AND KAUFMAN, A. 2002. Automatic centerline extraction for virtual colonoscopy. *IEEE Transactions on Medical Imaging* 21, 1450–1460.

WANG, G., AND VANNIER, M. W. 1995. Gi tract unraveling by spiral ct. *Proceedings SPIE 2434*, 307–315.

WANG, G., MCFARLAND, E. G., BROWN, B. P., AND VANNIER, M. W. 1998. Gi tract unraveling with curved cross section. *IEEE Transactions on Medical Imaging* 17, 318–322.

WANG, G., DAVE, S. B., BROWN, B. P., ZHANG, Z., MCFARLAND, E. G., HALLER, J. W., AND VANNIER, M. W. 1999. Colon unraveling based on electronic field: Recent progress and future work. *Proceedings SPIE 3660*, 125–132.

ZHANG, N., HONG, W., AND KAUFMAN, A. 2004. Dual contouring with topology-preserving simplification using enhanced cell representation. In *IEEE Visualization '04*, 505–512.

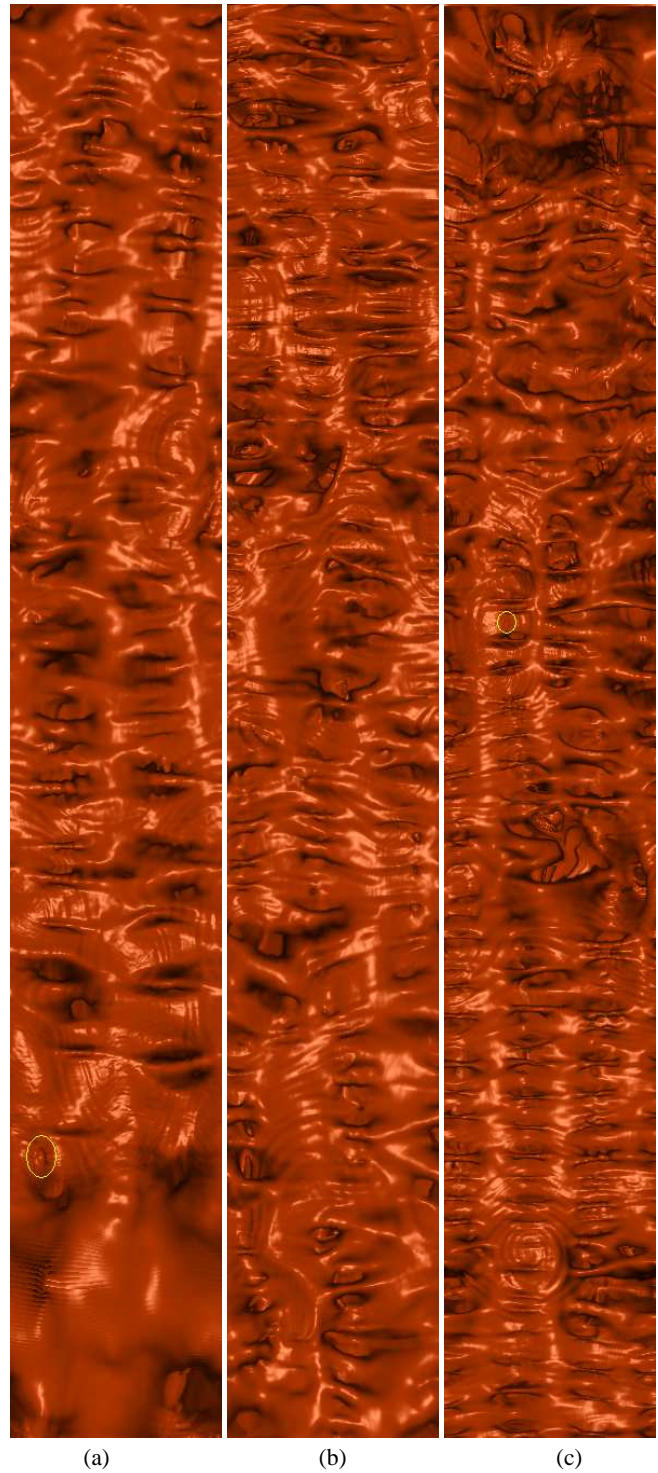


Figure 10: A flattened image for a whole colon data set is shown in three images. The bottom of the image (a) is the rectum of the colon, and the top of the image (c) is the cecum of the colon.